INSTITUTE OF PHYSICS PUBLISHING JOURNAL OF PHYSICS B: ATOMIC, MOLECULAR AND OPTICAL PHYSICS

J. Phys. B: At. Mol. Opt. Phys. **36** (2003) 319–329 PII: S0953-4075(03)54881-7

Angular correlation between Auger electrons successively emitted from photoexcited resonances in Kr and Xe

K Ueda[1,7], Y Shimizu[1,8], H Chiba[1], M Kitajima[2], M Okamoto[2], M Hoshino[2], H Tanaka[2], T Hayaishi[3], S Fritzsche[4], I P Sazhina[5] and N M Kabachnik[6,9]

[1] Institute of Multidisciplinary Research for Advanced Materials, Tohoku University, Sendai 980-8577, Japan
[2] Department of Physics, Sophia University, Tokyo 102-8554, Japan
[3] Institute of Applied Physics, University of Tsukuba, Tsukuba 305-8577, Japan
[4] Fachbereich Physik, Universität Kassel, 34132 Kassel, Germany
[5] Institute of Nuclear Physics, Moscow State University, 119899 Moscow, Russia
[6] Fakultät für Physik, Universität Bielefeld, 33615 Bielefeld, Germany

E-mail: ueda@tagen.tohoku.ac.jp

Received 10 October 2002, in final form 9 December 2002
Published 9 January 2003
Online at stacks.iop.org/JPhysB/36/319

Abstract

We have studied angular correlations between resonant Auger electrons and successive second-step Auger electrons emitted in a cascade decay after photoexcitation of resonances $3d_{5/2}^{-1}5p$ in Kr and $4d_{5/2}^{-1}6p$ in Xe. Two spectrometers were used for the angle-resolved detection of the two electrons in coincidence. Angular correlations for several pairs of strong lines have been measured in both atoms. The experimental results are compared with multiconfiguration Dirac–Fock calculations which include electron correlations in the initial, intermediate and final states of the cascade. In general, good agreement between experiment and theory is obtained.

1. Introduction

Electronic decay of core-excited atomic resonances has been intensively studied during the last decade (see review by Armen *et al* (2000) and references therein). Recent developments of synchrotron radiation sources contribute to the progress of these studies. The interest in the resonant Auger processes stems partly from the fact that electron–electron correlations play a decisive role in formation of the resonant Auger spectrum. In particular, the low-energy

[7] Author to whom any correspondence should be addressed.
[8] Present address: Miyazaki University, Miyazaki 889-2192, Japan.
[9] On leave from Institute of Nuclear Physics, Moscow State University, Moscow 119899, Russia.

part of these spectra has attracted interest because the majority of the low-energy transitions may lead also to highly excited ionic states with more than two open subshells. Owing to such shell structure most of these states are strongly correlated and hence require a mixture of many configurations in order to achieve an appropriate theoretical description. These states often decay further via Auger electron emission and thus a cascade of Auger transitions may be formed. The cascade in the resonant Auger decay determines the final charge distribution of the ions formed in the resonant photoabsorption.

The low-energy part of the electron spectra is often very complicated because it consists of a large number of partly overlapping lines which arise from the second-step Auger transitions as well as from the low-energy part of the first-step resonant Auger transitions. In this situation, coincidence spectroscopy may be successfully used for the proper identification of the lines and for studying the dynamics of the Auger cascades. A certain decay channel can be separated and identified by detecting two electrons in coincidence (von Raven *et al* 1990, von Raven 1992, Alkemper *et al* 1997). Even more detailed information can be obtained by measuring the angular correlations between the successively emitted electrons in the Auger cascade (Kabachnik 1997). Angle-resolved Auger-electron–Auger-electron coincidence experiments (Becker and Viefhaus 1996, Ueda *et al* 1999a, 2001, Wehlitz *et al* 1999, Turri *et al* 2001) have demonstrated that this technique provides a powerful method for studying both the line structure and dynamics of cascade Auger processes. A resonant state excited by a linearly polarized photon is aligned along the direction of the light polarization. The alignment causes an anisotropic angular distribution of the emitted resonant Auger electrons. Furthermore, the alignment is partly transferred to the intermediate ionic state populated in the first decay (see, e.g., Kabachnik *et al* 1999). Hence, the second-step Auger emission should also be anisotropic. Measurements of the angular distributions of the first- and second-step Auger electrons yield the anisotropy parameters β characterizing the emissions. If both electrons are detected in coincidence, then the angular distribution of the second electron is determined not only by the transferred alignment that is originally caused by the photon, but also by the alignment which appears as a result of emission of the first electron in a certain direction. The interplay between these two sources of anisotropy makes the angular correlation function much more complicated than the standard dipole-type angular distribution.

Recently we have published a series of measurements for spectra and angular distributions of the first- and second-step Auger emissions in the cascades following the resonant photoexcitations of rare gas atoms (Ueda *et al* 1999b, 2000, 2001, Yoshida *et al* 2000, Kitajima *et al* 2001, 2002). These measurements revealed strong lifetime interference effects in the Auger electron angular distributions as well as significant effects of configuration interaction. For resonantly excited argon, we also reported an angular correlation measurement following a $2p \rightarrow 4s$ excitation (Ueda *et al* 1999a, 2001) which helped to realize the so-called complete experiment for the resonant Auger decay, i.e. the experimental determination of the transition amplitudes and their phase differences (Ueda *et al* 1999a). In this paper, we report the results of angular correlation measurements in Auger cascades in Kr and Xe following the resonant excitation of the $3d_{5/2}^{-1}5p$ and $4d_{5/2}^{-1}6p$ states, respectively.

2. Experimental details

Details of the experimental setup and procedure have been described elsewhere (Ueda *et al* 2001) and thus only a brief account is given. The measurements were carried out at the Photon Factory, a 2.5 GeV synchrotron radiation facility in Japan. The beamline employed was the soft x-ray undulator beamline 16B where the 24 m spherical grating monochromator was installed (Shigemasa *et al* 1998). The photon energies used were 91.20 eV for the $3d_{5/2} \rightarrow 5p$

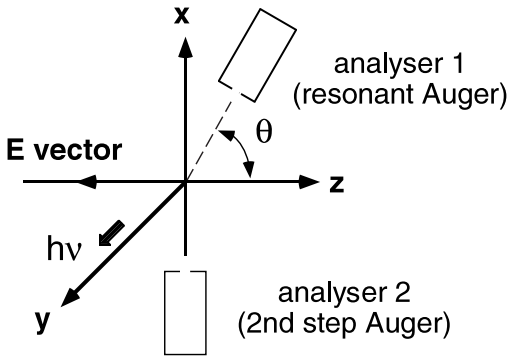

Figure 1. Experimental geometry.

excitation of Kr and 65.11 eV for the $4d_{5/2} \rightarrow 6p$ excitation of Xe. In both cases the photon bandwidths were set to ∼0.2 eV. The degree of linear polarization of the incident light was estimated to be $P_{\rm lin} = 100^{+0}_{-3}\%$ (Ueda *et al* 2001).

The experimental apparatus employed has been described elsewhere (Shimizu *et al* 1998). In the interaction region the focused photon beam was merged with an effusive gas beam. Figure 1 shows schematically the experimental geometry. The reaction plane was perpendicular to the photon beam. The first spectrometer was mounted on a turntable, whose axis of rotation was aligned to coincide with the incident light beam, and detected the resonant Auger electrons. The second spectrometer was set in such a way that it detected the electrons in the direction perpendicular to the linear polarization axis of the incident light, and detected the second-step Auger electrons. The energy bandwidths of these analysers were set to 0.2 eV. The coincidence rate between the first- and second-step electrons was measured as a function of the detection angle of the first-step resonant Auger electrons relative to the linear polarization axis of the incident light. The false coincidence rate was in general significantly smaller (typically $\leqslant 10\%$) than the true coincidence rate, and only the true coincidence rate was used in the analysis by subtracting off the false coincidence background. In order to remove the effect of the fluctuation of the coincidence counting rates as a function of time, we normalized the coincidence counts by the corresponding electron counts as detected by fixed analyser.

3. Theory and calculations

We assume that photoexcitation and electronic decay of a resonance and the following Auger decay of the ion can be considered as proceeding in a stepwise manner (Kabachnik 1997). This implies that well defined intermediate states exist with certain angular momenta and parity. A photoexcited resonant state $|J_0\rangle$ decays first to the intermediate state $|J_1\rangle$ (or group of states) with emission of a resonant Auger electron (first-step emission). Then the intermediate ionic state decays further to the final state $|J_2\rangle$ of the doubly ionized ion by emission of the second-step Auger electron. In all cases which are considered in this paper, the resonant state, i.e. the initial state of the first-step Auger decay, is an isolated resonance. After the first decay, a few intermediate states of the ion are populated. These intermediate states may partly overlap due to the lifetime width. In describing the second-step decay, therefore, the lifetime interference effect must be taken into account (Kabachnik *et al* 1994, Ueda *et al* 1999b). The corresponding expression for the angular correlation between two successively emitted electrons has been derived in our recent paper (Ueda *et al* 2001) on the basis of the general formalism (Kabachnik

et al 1999, Balashov *et al* 2000). Below we reproduce the basic expressions mainly for reference.

It is convenient to present the angular correlation function as an angular distribution of the second-step Auger electrons given that the first-step Auger electron is emitted in a certain direction $\boldsymbol{n}_1 \equiv \{\vartheta_1, \varphi_1\}$:

$$W(\boldsymbol{n}_1, \boldsymbol{n}_2) = \frac{c}{4\pi} \sum_{k_2 q_2 J_1 J_1'} A_{k_2}(J_1, J_1'; J_2) \rho_{k_2 q_2}(J_1, J_1'; \boldsymbol{n}_1) \gamma_{J_1 J_1'} (4\pi)^{1/2} \hat{k}_2^{-1} Y_{k_2 q_2}(\boldsymbol{n}_2). \tag{1}$$

Here $Y_{kq}(\boldsymbol{n})$ are spherical harmonics and factor $\gamma_{J_1 J_1'}$ results from the time averaging of the density matrix describing the interfering intermediate states

$$\gamma_{J_1 J_1'} = \frac{\Gamma_{J_1 J_1'} - \mathrm{i}\omega_{J_1 J_1'}}{\omega_{J_1 J_1'}^2 + \Gamma_{J_1 J_1'}^2}, \tag{2}$$

where $\omega_{J_1 J_1'} = E_{J_1} - E_{J_1'}$ is the energy splitting of the overlapping states with total angular momenta J_1 and J_1' which are populated after the first decay; $\Gamma_{J_1 J_1'} = \frac{1}{2}(\Gamma_{J_1} + \Gamma_{J_1'})$ with Γ_{J_1} being the total width of the level J_1. The normalization constant c in equation (1) is irrelevant to the considered angular distributions. An alternative expansion in terms of bipolar harmonics was used by Kabachnik (1992), Schmidt (1997) and Turri *et al* (2001).

The generalized anisotropy coefficients $A_{k_2}(J_1, J_1'; J_2)$ can be expressed in terms of the Auger amplitudes $\langle J_2, l_2 j_2 \| V \| J_1 \rangle$, which characterize the second-step Auger decay (Kabachnik *et al* 1994):

$$\begin{aligned} A_{k_2}(J_1, J_1'; J_2) = (-1)^{J_1 + J_2 - 1/2} \sum_{l_2 l_2' j_2 j_2'} & \hat{l}_2 \hat{l}_2' \hat{j}_2 \hat{j}_2' \hat{J}_1 \hat{J}_1' (l_2 0, l_2' 0 | k_2 0) \\ & \times \begin{Bmatrix} l_2 & j_2 & \frac{1}{2} \\ j_2' & l_2' & k_2 \end{Bmatrix} \begin{Bmatrix} J_1 & j_2 & J_2 \\ j_2' & J_1' & k_2 \end{Bmatrix} \langle J_2, l_2 j_2 \| V \| J_1 \rangle \langle J_2, l_2' j_2' \| V \| J_1' \rangle^*. \end{aligned} \tag{3}$$

Here we use standard notation for the Clebsch–Gordan and Wigner $6j$ coefficients: $\hat{J} \equiv \sqrt{2J+1}$; l_2 and j_2 are the orbital and total angular momenta of the second-step Auger electron, respectively.

The differential statistical tensors for the intermediate states $\rho_{k_2 q_2}(J_1, J_1'; \boldsymbol{n}_1)$ describe their anisotropy when the first electron is detected in direction $\boldsymbol{n}_1$:

$$\begin{aligned} \rho_{k_2 q_2}(J_1, J_1'; \boldsymbol{n}_1) = \sum_{k_0 q_0 k_1 q_1} & (4\pi)^{1/2} \hat{k}_2 \hat{J}_0 \hat{J}_1^{-1} (k_1 q_1, k_2 q_2 | k_0 q_0) \rho_{k_0 q_0}(J_0, J_0) \\ & \times Y_{k_1 q_1}(\boldsymbol{n}_1) B_{k_1 k_2 k_0}(J_0; J_1, J_1'). \end{aligned} \tag{4}$$

Here $\rho_{k_0 q_0}(J_0, J_0)$ are the statistical tensors describing the polarization state of the resonance $|J_0\rangle$. When it is excited from the closed-shell ground state by linearly polarized light (the z-axis is chosen along the light polarization), only two components are non-zero: $\rho_{00}(J_0, J_0) = 1/\sqrt{3}$ and $\rho_{20}(J_0, J_0) = -\sqrt{2/3}$. The factors $B_{k_1 k_2 k_0}(J_0; J_1, J_1')$ are given by the relation (Kabachnik *et al* 1999)

$$\begin{aligned} B_{k_1 k_2 k_0}(J_0; J_1, J_1') = (-1)^{k_1 - k_0} (4\pi)^{-1} \hat{J}_0 \hat{J}_1 \sum_{l_1 l_1' j_1 j_1'} & (-1)^{j_1' + \frac{1}{2}} \hat{l}_1 \hat{l}_1' \hat{j}_1 \hat{j}_1' \\ & \times (l_1 0, l_1' 0 | k_1 0) \begin{Bmatrix} l_1 & j_1 & \frac{1}{2} \\ j_1' & l_1' & k_1 \end{Bmatrix} \begin{Bmatrix} J_1 & j_1 & J_0 \\ J_1' & j_1' & J_0 \\ k_2 & k_1 & k_0 \end{Bmatrix} \\ & \times \langle J_1, l_1 j_1 \| V \| J_0 \rangle \langle J_1', l_1' j_1' \| V \| J_0 \rangle^*, \end{aligned} \tag{5}$$

where standard notation for the Wigner $6j$ and $9j$ coefficients is used and $\langle J_1, l_1 j_1 \| V \| J_0 \rangle$ denotes the decay amplitude which describes the first-step resonant Auger transition from the

initial state $|J_0\rangle$ to the intermediate state $|J_1\rangle$ by emission of an electron with the orbital and total angular momenta l_1 and j_1, respectively.

Due to parity conservation in both decays the values of k_1 and k_2 are even. Besides, $k_2 \leqslant 2J_1$. In the particular cases considered below, the maximum value of the angular momenta of the intermediate states is $J_1 = 5/2$ and thus the summation over k_2, q_2 in equation (1) is limited by the conditions $k_2, q_2 \leqslant 4$. For the chosen geometry of the experiment (see figure 1) and with the z-axis directed along the light polarization, we have $\boldsymbol{n}_1 = \{\vartheta_1, 0\}$ and $\boldsymbol{n}_2 = \{\frac{3\pi}{2}, 0\}$. Then, from the properties of spherical harmonics it follows that in the given geometry q_1 and q_2 are both even.

Since in photoabsorption the rank of the statistical tensor $\rho_{k_0 q_0}(J_0, J_0)$ is limited by $k_0 \leqslant 2$, it follows from the properties of the Clebsch–Gordan coefficients in equation (4) that $k_1 \leqslant 6$. Therefore, the angular distribution (1) with (4) contains even spherical harmonics up to the sixth order and, in the particular geometry of figure 1, may be expressed in the following form:

$$W(\vartheta_1) = \sum_{i=0}^{3} a_{2\mathrm{i}} \cos(2\mathrm{i}\vartheta_1). \tag{6}$$

The coefficients $a_{2\mathrm{i}}$ are determined by A_{k_2} and $B_{k_1 k_2 k_0}$ which can be evaluated according to equations (3) and (5) in terms of the Auger amplitudes.

The Auger amplitudes of the first- and second-step transitions have been calculated within the multiconfiguration Dirac–Fock (MCDF) method. Since the details of the computations and, in particular, the choice of the configuration state functions (CSFs) have been discussed in our previous investigations for Kr and Xe (Kitajima *et al* 2001, 2002), only a brief account will be given in the following. The bound state wavefunctions have been calculated using the relativistic atomic structure code GRASP92 (Parpia *et al* 1996). The initial resonant states $3d_{5/2}^{-1}5p$ in Kr and $4d_{5/2}^{-1}6p$ in Xe are well described within the single (non-relativistic) configuration approximation. The intermediate ionic states and the final states of the doubly charged ions exhibit a strong mixing of configurations. In order to describe the intermediate states, we include all CSFs with total angular momenta $J = 1/2, \ldots, 7/2$ from $ns^1np^5(n+1)p$ configuration as well as the $J = 1/2$ and $3/2$ levels from $ns^0np^6(n+1)p$ and $ns^2np^3nd(n+1)p$ configurations ($n = 4$ for Kr and 5 for Xe), as in our previous studies (Kitajima *et al* 2001, 2002). A total of 194 CSFs constitute the basis of the wavefunction expansion of the intermediate state. The final states of the cascade were obtained in a basis of 106 CSFs with angular momenta $J = 0$, 1 and 2 including the four configurations ns^1np^5, ns^2np^4, $ns^2np^2nd^2$ and $ns^2np^2(n+1)p^2$.

The continuum wavefunctions were calculated by solving the Dirac–Fock equations in the static field of the final bound state (for each transition) including the exchange interaction with the bound electrons. Both these continuum orbitals as well as the Auger amplitudes were obtained using the program RATIP (Fritzsche 2001). Once the amplitudes were known the coefficients $A_{k_2}(J_1, J_1'; J_2)$, equation (3), and $B_{k_1 k_2 k_0}(J_0; J_1, J_1')$, equation (5), were calculated by means of the RACAH package (Fritzsche 1997, Fritzsche *et al* 2001) for each of the selected cascades of the Auger transitions and finally the angular correlation functions were obtained.

4. Results and discussion

4.1. Auger cascades in Kr

The angular correlations have been measured for the following cascades of Auger transitions in Kr (corresponding kinetic energies of electrons are shown in parentheses):

(a) $3d_{5/2}^{-1}5p$ ($J_0 = 1$) $\rightarrow$ $4s^14p^5(^1P)5p \rightarrow 4s^24p^4\ ^1D_2$ (lines 43.00 and 8.03 eV);
(b) $3d_{5/2}^{-1}5p$ ($J_0 = 1$) $\rightarrow$ $4s^14p^5(^1P)5p \rightarrow 4s^24p^4\ ^3P_2$ (lines 43.00 and 9.85 eV);
(c) $3d_{5/2}^{-1}5p$ ($J_0 = 1$) $\rightarrow$ $4s^14p^5(^1P)5p \rightarrow 4s^24p^4\ ^3P_1$ (lines 43.00 and 9.29 eV);
(d) $3d_{5/2}^{-1}5p$ ($J_0 = 1$) $\rightarrow$ $4s^24p^34d(^1P)5p \rightarrow 4s^24p^4\ ^1D_2$ (lines 36.74 and 14.26 eV);
(e) $3d_{5/2}^{-1}5p$ ($J_0 = 1$) $\rightarrow$ $4s^04p^6(^1S)5p \rightarrow 4s^14p^5\ ^3P_2$ (lines 29.25 and 9.22 eV).

Note that the total spin and orbital angular momentum quantum numbers in the notation ^{2S+1}L should be considered as only a label since the real states as well as the calculated states are mixtures of all possible L and S. The experimental results are shown in figure 2, where they are compared with the calculated angular correlation functions. In general, the agreement is good.

It is of interest to understand which factors determine the angular correlation pattern, why the patterns are so different for different transitions, and if it is possible to predict the patterns on the basis of simple models like a spectator model for the resonant Auger decay or a pure LSJ-coupling model. First, consider the first three cascades (a)–(c). These show very different angular correlation patterns (see figure 2), although the same intermediate states, $4s^14p^5(^1P)5p^2,\ ^2P\ ^2D$, are involved. We note that, although several closely lying intermediate states are populated in these cascades, the transition to the state $J_1 = 5/2$, which may be denoted as $4s^14p^5(^1P)5p\ ^2D_{5/2}$, strongly dominates. In the following qualitative discussion, therefore, we take into account only this intermediate state.

According to expression (1), the angular correlation function can be considered as an angular distribution of the second-step Auger electron emission from an anisotropic intermediate ion produced in the first-step decay. The anisotropy of the ion is determined by two factors. One is the alignment induced by the photon and partly transferred to the intermediate ionic state. This alignment is described by the second-rank statistical tensor $\rho_{20}(J_0, J_0)$ and refers to the axis determined by the photon polarization. If only this factor was important, the correlation function would have been of the typical dipole-type shape $1 + \beta P_2(\cos\vartheta)$. However, there is a second source of the anisotropy, namely the alignment produced by emission of the first-step Auger electron. This alignment exists, even if $\rho_{20}(J_0, J_0) = 0$. It has a natural axis: the direction of the electron emission. The shape of the correlation pattern in cases (b) and (c) clearly indicate the presence of terms with $i > 2$ in expansion (6). This means that the second factor is important. Moreover, the calculations show that the term proportional to $\cos(6\vartheta)$ is large. This term can appear only as a result of a combination of both alignments. Therefore, the anisotropy produced by photoabsorption and by Auger electron emission are equally important and their interplay determines the anisotropy of the intermediate ionic state. On the other hand, the angular patterns for transitions (a) and (c) from the same intermediate state are strikingly different. This illustrates that the intrinsic anisotropy parameters $\alpha_k = A_k(J_1, J_1'; J_2)/A_0(J_1, J_1'; J_2)$, which describe the second-step decay and characteristic for each particular decay channel, are also important for predicting the angular correlations.

In the first-step transitions of cascades (a)–(c), the ϵp and ϵf Auger electron partial waves are allowed by the angular momentum and parity conservation laws. Therefore, in general, the corresponding Auger amplitudes are necessary for the calculations of the anisotropy of the intermediate ion. However, as was shown by previous calculations (Tulkki *et al* 1994, Mursu *et al* 1998, Kitajima *et al* 2001), the Auger partial wave $\epsilon f_{7/2}$ strongly dominates for the transition to the $4s^14p^5(^1P)5p\ ^2D_{5/2}$ state considered here. If we suppose that only one partial wave contributes to the decay (single-channel approximation), then all $B_{k_1k_2k_0}(J_0; J_1, J_1')$ coefficients and therefore the statistical tensors of the intermediate state (4) can be evaluated to

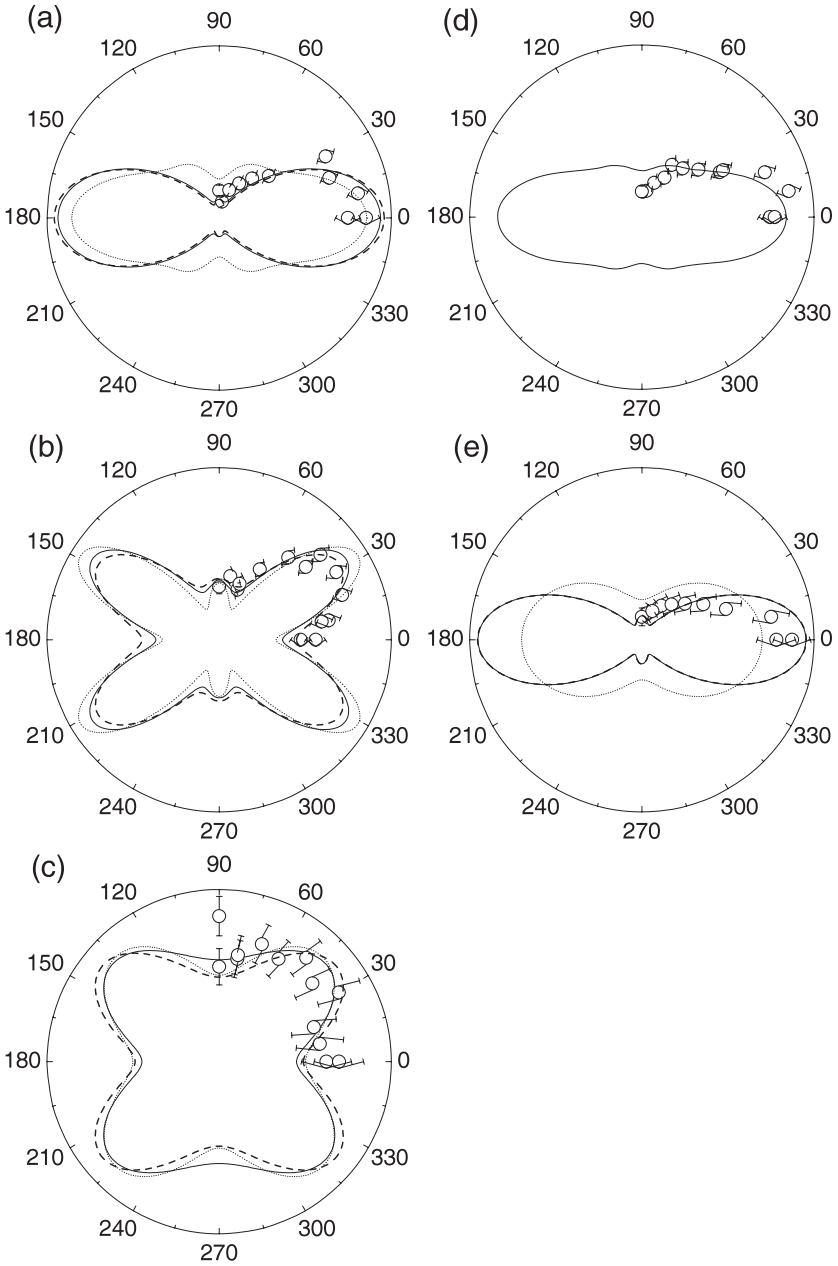

Figure 2. Angular correlation between the resonant Auger emission and the second-step Auger emission for the Kr transitions (a) $3d_{5/2}^{-1}5p$ ($J_0 = 1$) $\rightarrow$ $4s^14p^5(^1P)5p \rightarrow 4s^24p^4\ ^1D_2$; (b) $3d_{5/2}^{-1}5p$ ($J_0 = 1$) $\rightarrow$ $4s^14p^5(^1P)5p \rightarrow 4s^24p^4\ ^3P_2$; (c) $3d_{5/2}^{-1}5p$ ($J_0 = 1$) $\rightarrow$ $4s^14p^5(^1P)5p \rightarrow 4s^24p^4\ ^3P_1$; (d) $3d_{5/2}^{-1}5p$ ($J_0 = 1$) $\rightarrow$ $4s^24p^34d(^1P)5p \rightarrow 4s^24p^4\ ^1D_2$; (e) $3d_{5/2}^{-1}5p$ ($J_0 = 1$) $\rightarrow$ $4s^04p^6(^1S)5p \rightarrow 4s^14p^5\ ^3P_2$. Coincidence rates are plotted as a function of the angle of the direction of first-step Auger electron relative to the polarization vector whereas the second-step Auger electron is detected in the direction at 270° (see figure 1). The solid curves represent the results of the MCDF calculation. The dashed and dotted curves correspond to the calculations with only one partial wave in the first-step emission and MCDF and LSJ-coupling approximation for the second-step transitions, respectively. Theoretical curves are normalized to the same area limited by the curves.

Table 1. The calculated intrinsic anisotropy parameters α_k for some second-step Auger electron transitions from the $4s^1 4p^5 (^1P) 5p\ ^2D_{5/2}$ and $4s^0 4p^6 (^1S) 5p\ ^2P_{3/2}$ intermediate states of Kr^+ ion. The values have been obtained in the MCDF calculation described in the text and in the LSJ-coupling approximation. The values marked by asterisks have been calculated considering the d-wave only (see text).

Initial state	Final state	α_2		α_4	
		MCDF	LSJ	MCDF	LSJ
$4s^1 4p^5 (^1P) 5p\ ^2D_{5/2}$	$4p^4\ ^3P_2$	−0.400	−0.382	−0.583	−1.058
	$4p^4\ ^3P_1$	−0.686	−0.748	−0.180	0
	$4p^4\ ^1D_2$	−0.719	0.229*	−0.052	0.264*
$4s^0 4p^6 (^1S) 5p\ ^2P_{3/2}$	$4s4p^5\ ^3P_2$	0.765	0*	0	0

a constant factor without calculation of the Auger amplitudes. We made this calculation with an additional assumption that the interference of the considered level with its neighbours is negligible. The latter assumption is justified because the considered transition is much stronger than those to the neighbouring levels. The angular pattern was then calculated with the α_k parameters taken from our full configuration interaction calculations (see table 1). The results are shown in figures 2(a)–(c) by the dashed curves. Each curve is normalized to the same area limited by the curve. The difference from the exact calculation is small. This confirms that the $\epsilon f_{7/2}$ partial wave is indeed dominant. It also shows that in this case the anisotropy of the intermediate level is practically independent of any model used for the description of the resonant and intermediate states because the Auger amplitudes cancel out of the final expression.

In contrast, the intrinsic anisotropy parameters for the second-step Auger transitions are strongly model-dependent. In the second step of the considered cascades (a)–(c), only even partial waves ($\epsilon s, \epsilon d$ and ϵg) can contribute. If we assume that the LSJ-coupling approximation is valid for the intermediate and final states, then, in the decays to the ^3P states, (b) and (c), only the d-wave contributes (Kabachnik and Sazhina 1988). The resulting α_k parameters shown in table 1 considerably deviate from our MCDF calculation. A decay to the ^1D final state (a) is described by at least two channels ϵs and ϵd even in the LSJ-coupling model and in the single-configuration approximation. The large observed anisotropy may suggest that the contribution of the d-wave could be significant. However, if we make the assumption that only the d-wave contributes, the resulting intrinsic parameters are far from the MCDF results (see table 1) and the angular correlation function shown by dotted curve in figure 2(a) is far from the experiment. The reason for the large discrepancy of the simple model and the MCDF calculation is that the intermediate state $4s^1 4p^5 (^1P) 5p\ ^2D_{5/2}$ is in fact described by a strong mixture of configurations with the dominant configuration $4s^2 4p^3 4d5p$ which can allow the g-wave emission forbidden for the title configuration in the single configuration approximation. The large contribution of the g-wave changes drastically the α_k parameters and gives rise to a good agreement with experiment.

It is interesting to compare the angular correlations in the cascades (a) and (d) which start and finish at the same states but proceed through different intermediate states. In case (d) the first-step transition is a so-called correlation satellite of the transition in (a). The state with configuration $4s^2 4p^3 4d(^1P) 5p$ cannot be populated directly from the resonant state $3d_{5/2}^{-1} 5p$ since more than two electrons need to participate in the transition. Therefore, the intermediate state in case (d) is populated due to admixture of the $4s^1 4p^5 (^1P) 5p$ diagram configuration. This should lead to a strong similarity of the alignment of intermediate states in both cascades.

The observed (and calculated) difference in angular correlation may be connected only with the different α_k coefficients. In the second-step decay both components of the configuration expansion participate and thus the Auger amplitudes depend on their relative strength. In our MCDF calculations for the case (d) the anisotropy parameters of the second-step decay are $\alpha_2 = 0.317$ and $\alpha_4 = 0.212$. Accidentally, these values are close to those calculated in LSJ-coupling for the case (a) (see table 1). Because of this, the angular correlation function figure 2(d) is similar to the curve in figure 2(a).

The cascade (e) is different from the first four cascades since it proceeds through the intermediate state of odd parity and therefore involves partial waves ϵs and ϵd in the first-step as well as in the second-step transitions. The ^{2}P intermediate states can be described by statistical tensors with maximal rank $k_2 = 2$. Thus $k_1 \leqslant 4$ and the terms up to $\cos(4\vartheta_1)$ can appear in the expansion (6). Within a spectator model, the $\epsilon d_{5/2}$ is the only possible partial electronic wave in the first-step transition $3d_{5/2}^{-1}5p$ ($J_0 = 1$) $\rightarrow$ $4s^0 4p^6(^1S)5p$. Our MCDF calculation indeed confirms that the $d_{5/2}$ partial wave strongly dominates. Therefore, we can calculate the statistical tensors of the intermediate state $^2P_{3/2}$ in the single-channel approximation, as we did it for the cases (a)–(c). For the second-step transition to the $^3P_2$ state, the anisotropy parameter α_2 crucially depends on the relative contribution of ϵs and ϵd waves. Note that $\alpha_4 = 0$ in this case. It is interesting to note that $\alpha_2 = 0$ in the LSJ approximation if only one of the partial waves contributes (Kabachnik and Sazhina 1984). The MCDF calculation gives $\alpha_2 = 0.765$. With this value and with the statistical tensors calculated in the single-channel ($d_{5/2}$) approximation we have obtained the result shown by the dashed line in figure 2(e) which is very close to the full MCDF calculation. For comparison, we show by the dotted line an analogous result but with $\alpha_2 = 0$. This result corresponds to the LSJ approximation with the dominance of the s- or d-wave. One can see that the latter curve considerably deviates from the first two. Therefore, as in the cases (a)–(c) above, the angular correlation function is more sensitive to the anisotropy parameter of the second-step transition than to the description of the first step where only one partial wave dominates.

Concluding our discussion, we note that the coincidence experiment is much more sensitive to the details of the description of the second step transition than the corresponding non-coincidence measurement (Kitajima *et al* 2001). The explanation of this difference lies in the fact that the alignment transfer to the intermediate state in the non-coincidence experiment is very small (Ueda *et al* 2000) and the resulting anisotropy of the second-step Auger emission is difficult to measure with the precision which is necessary for determining the intrinsic parameters α_k.

4.2. Auger cascades in Xe

In Xe the following cascades of Auger transitions have been studied (the corresponding kinetic energies of electrons are shown in parentheses):

(a) $4d_{5/2}^{-1}6p$ ($J_0 = 1$) $\rightarrow$ $5s^1 5p^5(^1P)6p \rightarrow 5s^2 5p^4\ ^1D_2$ (lines 24.38 and 5.52 eV);
(b) $4d_{5/2}^{-1}6p$ ($J_0 = 1$) $\rightarrow$ $5s^1 5p^5(^1P)6p \rightarrow 5s^2 5p^4\ ^3P_2$ (lines 24.38 and 7.64 eV);
(c) $4d_{5/2}^{-1}6p$ ($J_0 = 1$) $\rightarrow$ $5s^0 5p^6(^1S)6p \rightarrow 5s^1 5p^5\ ^3P_2$ (lines 12.99 and 6.86 eV);
(d) $4d_{5/2}^{-1}6p$ ($J_0 = 1$) $\rightarrow$ $5s^0 5p^6(^1S)6p \rightarrow 5s^1 5p^5\ ^3P_1$ (lines 12.99 and 6.20 eV).

The experimental data as well as the results of calculations are shown in figure 3. One sees that for xenon the agreement between theory and experiment is still satisfactory, although somewhat worse than for krypton. Good agreement is obtained for the cascades (a) and (c), while for (b) and (d) the shape of the experimental curve differs from the calculated one. A possible

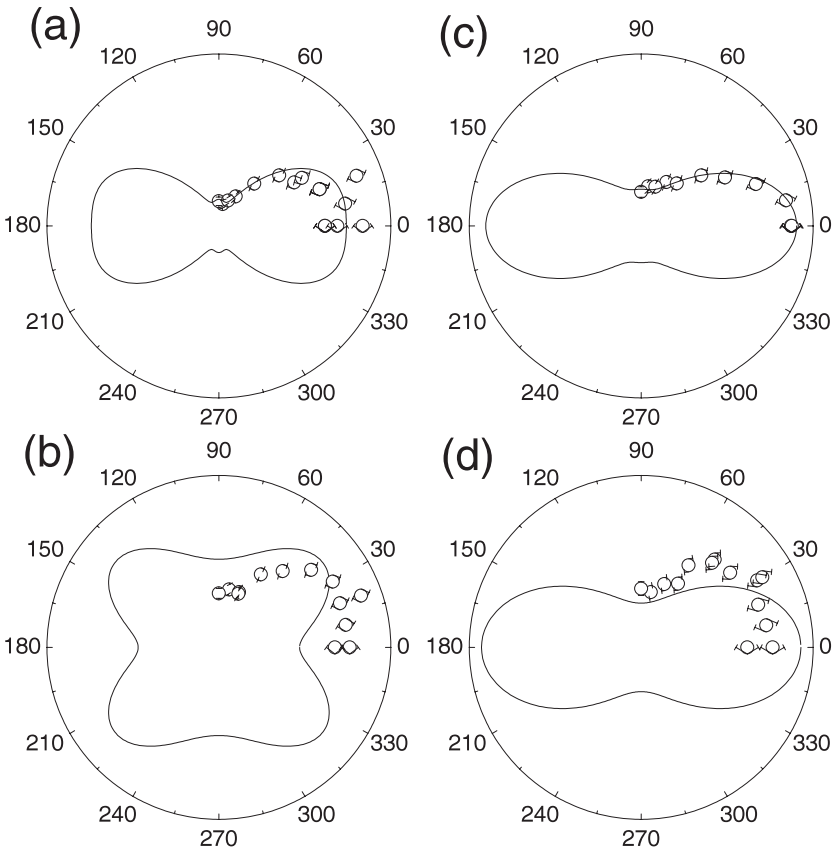

Figure 3. Angular correlation between the resonant Auger emission and the second-step Auger emission for the Xe transitions (a) $4d_{5/2}^{-1}6p$ ($J_0 = 1$) $\rightarrow$ $5s^15p^5(^1P)6p \rightarrow 5s^25p^4\ ^1D_2$; (b) $4d_{5/2}^{-1}6p$ ($J_0 = 1$) $\rightarrow$ $5s^15p^5(^1P)6p \rightarrow 5s^25p^4\ ^3P_2$; (c) $4d_{5/2}^{-1}6p$ ($J_0 = 1$) $\rightarrow$ $5s^05p^6(^1S)6p \rightarrow 5s^15p^5\ ^3P_2$; (d) $4d_{5/2}^{-1}6p$ ($J_0 = 1$) $\rightarrow$ $5s^05p^6(^1S)6p \rightarrow 5s^15p^5\ ^3P_1$. Coincidence rates are plotted as a function of the angle of the direction of first-step Auger electron relative to the polarization vector whereas the second-step Auger electron is detected in the direction at 270° (see figure 1). The curves represent the results of the MCDF calculation.

explanation of the worse agreement between theory and experiment for Xe as compared to Kr is a higher density of spectral lines in the Xe case which makes it difficult to separate the lines in the coincidence experiment. The considered cascades in Xe are very similar to the corresponding cascades in Kr and, hence, our qualitative consideration, as presented above, remains valid also for xenon. The angular correlation patterns are very sensitive to the anisotropy parameters of the second-step Auger transitions.

5. Conclusion

The angular correlations between two successively emitted Auger electrons have been measured for several strong lines in the decay of the photoexcited $3d_{5/2}^{-1}5p$ resonance in Kr and the $4d_{5/2}^{-1}6p$ resonance in Xe. The shape of the angular correlation pattern is determined by both the transfer of photo-induced alignment and the alignment due to the emission of the first electron. In the majority of the considered cases, the calculations based on the MCDF

approach reproduce the experimental results well. We have found that the shape of the angular patterns is very sensitive to the intrinsic anisotropy parameters of the second-step Auger decay. The coincidence experiments provide a unique opportunity to study anisotropy of the Auger transitions in ions, because, in non-coincidence measurements, it is difficult to measure these parameters due to a very small alignment transfer to the intermediate states.

Acknowledgments

The experiment was carried out with the approval of the Photon Factory Advisory Committee (proposal no 98G231). The authors are grateful to the staff of the Photon Factory for their help in the course of the experiment. NMK acknowledges the hospitality of Bielefeld University and the financial support by the Deutsche Forschungsgemeinschaft (DFG) within the Mercator professorship programme.

References

Alkemper U, Doppelfeld J and von Busch F 1997 *Phys. Rev.* A **56** 2741
Armen G B, Aksela H, Åberg T and Aksela S 2000 *J. Phys. B: At. Mol. Opt. Phys.* **33** R49
Balashov V V, Grum-Grzhimailo A N and Kabachnik N M 2000 *Polarization and Correlation Phenomena in Atomic Collisions. A Practical Theory Course* (New York: Kluwer) ch 3
Becker U and Viefhaus J 1996 *Selected Topics on Electron Physics* ed Campbell and H Kleinpoppen (New York: Plenum) p 333
Fritzsche S 1997 *Comput. Phys. Commun.* **103** 51
Fritzsche S 2001 *J. Electron Spectrosc. Relat. Phenom.* **114–116** 1155
Fritzsche S, Inghoff T, Bastug T and Tomaselli M 2001 *Comput. Phys. Commun.* **139** 314
Kabachnik N M 1992 *J. Phys. B: At. Mol. Opt. Phys.* **25** L389
Kabachnik N M 1997 *X-ray and Inner-Shell Processes* vol 389, ed R J Johnson, H Schmidt-Böcking and B F Sonntag (New York: American Institute of Physics) p 689
Kabachnik N M and Sazhina I P 1984 *J. Phys. B: At. Mol. Phys.* **17** 1335
Kabachnik N M and Sazhina I P 1988 *J. Phys. B: At. Mol. Opt. Phys.* **21** 267
Kabachnik N M, Sazhina I P and Ueda K 1999 *J. Phys. B: At. Mol. Opt. Phys.* **32** 1769
Kabachnik N M, Tulkki J, Aksela H and Ricz S 1994 *Phys. Rev.* A **49** 4653
Kitajima M *et al* 2001 *J. Phys. B: At. Mol. Opt. Phys.* **34** 3829
Kitajima M, Okamoto M, Hoshino M, Tanaka H, Fritzsche S, Kabachnik N M, Sazhina I P, Shimizu Y and Ueda K 2002 *J. Phys. B: At. Mol. Opt. Phys.* **35** 3327
Mursu J, Jauhiainen J, Aksela H and Aksela S 1998 *J. Phys. B: At. Mol. Opt. Phys.* **31** 1973
Parpia F A, Froese Fischer C and Grant I P 1996 *Comput. Phys. Commun.* **94** 249
Schmidt V 1997 *Electron Spectrometry of Atoms Using Synchrotron Radiation* (New York: Cambridge University Press) ch 4
Shigemasa E, Toyoshima A, Yan Y, Hayaishi T, Soejima K, Kiyokura T and Yagishita A 1998 *J. Synchrotron Radiat.* **5** 777
Shimizu Y *et al* 1998 *J. Electron Spectrosc. Relat. Phenom.* **88–91** 1031
Tulkki J, Aksela H and Kabachnik N M 1994 *Phys. Rev.* A **50** 2366
Turri G, Battera G, Avaldi L, Camilloni R, Coreno M, Ruocco A, Colle R, Simonucci S and Stefani G 2001 *J. Electron Spectrosc. Relat. Phenom.* **114–116** 199
Ueda K, Kabachnik N M, Kitajima M, Okamoto M, Shimizu Y, Chiba H, Hayaishi T and Tanaka H 2000 *J. Phys. B: At. Mol. Opt. Phys.* **33** L475
Ueda K, Shimizu Y, Chiba H, Kitajima M, Tanaka H, Fritzsche S and Kabachnik N M 2001 *J. Phys. B: At. Mol. Opt. Phys.* **34** 107
Ueda K, Shimizu Y, Chiba H, Sato Y, Kitajima M, Tanaka H and Kabachnik N M 1999a *Phys. Rev. Lett.* **83** 5463
Ueda K, Shimizu Y, Kabachnik N M, Sazhina I P, Wehlitz R, Becker U, Kitajima M and Tanaka H 1999b *J. Phys. B: At. Mol. Opt. Phys.* **32** L291
von Raven E 1992 *Thesis* Hamburg University unpublished
von Raven E, Meyer M, Pahler M and Sonntag B 1990 *J. Electron Spectrosc. Relat. Phenom.* **52** 677
Wehlitz R, Pibida L S, Levin J C and Sellin I A 1999 *Phys. Rev.* A **59** 421
Yoshida H *et al* 2000 *J. Phys. B: At. Mol. Opt. Phys.* **33** 4343